

## **Compact Force Sensors for Low-Force Mechanical Probe Calibration**

Douglas T. Smith, Shane Woody, and Jon R. Pratt  
National Institute of Standards and Technology (NIST), Gaithersburg, MD USA

### **Abstract**

The loading mechanisms of instrumented indentation machines are often calibrated using deadweights. In many cases, due to the geometry of the loading frame, the applied deadweight is tensile, while the indentation loads to be measured are compressive. In this paper, we report preliminary efforts to develop a compressive load cell for use on a typical instrumented indentation machine. Two devices were evaluated, one a compact capacitance-based device (fabricated at the National Institute of Standards and Technology), the other a piezoresistive force sensor. We will describe the calibration sensitivity, stability and drift of each, and discuss the potential use of each as a force transfer artifact for the calibration of instrumented indenters.

### **Introduction**

The use of mechanical testing devices with forces in the millinewton, micronewton, and nanonewton ranges has grown dramatically in the last ten years. This growth is primarily within the atomic force microscope (AFM) and nanoindenter communities, but the need to apply and measure small forces arises in other areas, such as micro-electro-mechanical systems (MEMS), as well. The increased use of nanoindentation in particular for routine testing of the mechanical properties of coatings and thin films has led to the drafting of several testing standards (ISO Draft International Standard DIS 14577 and draft documents in ASTM Task Group E28.06.11, for example) that will require traceable force calibration of testing machines. Accurate calibration of low-force devices remains a challenge, however, as the uncertainty in mass artifacts increases significantly for masses less than one gram. A compact, accurate force calibration system, traceable to a primary force standard in these ranges, is needed.

The National Institute of Standards and Technology (NIST) currently has a program underway that is developing both primary realizations of force in these ranges as well as force transfer devices (load cells) that can be used for field calibration of mechanical test equipment [1]. The work presented here focuses on transfer devices. Preliminary results are presented for two different force calibration devices, one a capacitance cell, the other a silicon beam with integral piezoresistive measurement of strain. The work on the silicon beam is similar to recent work on force measurement with micromechanical beams [2] and the use of a nanoindenter to measure spring constants of AFM cantilevers [3], but here the emphasis is on the accuracy, stability and traceability of the transfer device.

### **Experimental**

The capacitance cell was designed and constructed at NIST. The device is essentially a cantilevered beam of borosilicate microscope cover slip glass, 160  $\mu\text{m}$  thick, mounted 50  $\mu\text{m}$  above a fixed counter-electrode also made of borosilicate glass. Both electrode surfaces received a thermally evaporated Au coating, with a thin Cr interlayer as an

adhesion promoter. The cantilevered beam was attached to a shoulder on the counter-electrode base with a fast-curing epoxy, placed only around the contact edges while the two surfaces are clamped together. The free area of the cantilevered beam is 20 mm wide by 15 mm long. A small Macor washer was epoxied to the top surface of the beam, at the center of its free area, and a small brass platen was inserted into this washer to serve as a force application point. This assembly was then mounted in a brass enclosure, which is shown in Figure 1. The brass platen can be seen protruding slightly through an opening in the top surface.

The capacitance of the cell was measured with a precision 1 kHz capacitance bridge. For capacitances below 100 pF, this bridge has a resolution of  $0.5 \times 10^{-6}$  pF and an estimated standard uncertainty of  $15 \times 10^{-6}$  pF. With no external applied force, the capacitance of the cell had a nominal value of 43 pF. Its sensitivity to force was found to be approximately 0.124 pF/mN.

The force sensor element studied in this work was a SensoNor AE801 sensor element (SensorOne, Sausalito, CA, USA). It consists of a rectangular silicon beam, 5.0 mm long, 0.95 mm wide and 0.15 mm thick. Near the mounting end, it contains two piezoresistive strain gauge elements, one each on the top and bottom face, which are created using ion implantation. Figure 2 is a composite micrograph of one face, showing a resistive element and, at the far right, the ends of the contact electrodes, which also serve as the mechanical mounts for the beam. The manufacturer specifies that each resistive element will have a resistance of approximately 1 k $\Omega$ , and that the beam will have a spring constant of 2 N/m for forces applied at its end. We found the two resistive elements to have values of 1098  $\Omega$  and 1101  $\Omega$ . Values for beam stiffness are discussed below.

For the work described here, the relative change in resistance of the two elements in response to loading of the beam was measured by placing them in a standard Wheatstone bridge configuration, with a 1.0 kHz, 1.00 V(rms) AC excitation voltage and manual balancing via a 10  $\Omega$  resistor trim pot between two precision fixed resistors. The bridge detector was a lock-in amplifier. Data from both the lock-in and the capacitance bridge were logged by a standard personal computer using a GPIB interface.



**Figure 1.** Capacitance cell showing the external leads to the upper and lower electrodes. The mass platen is visible through a hole in the top surface.

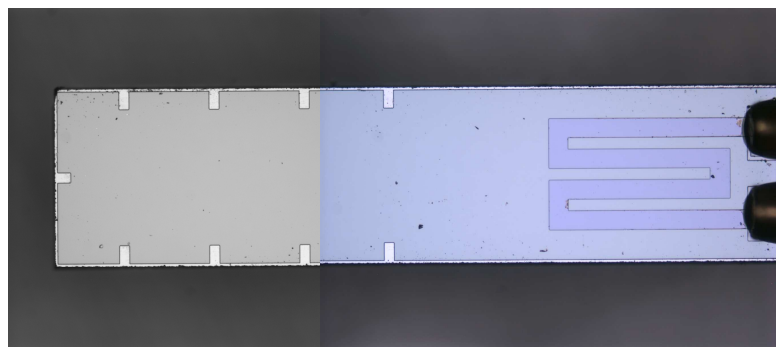


**Figure 2.** A composite of two micrographs, taken with a 5x objective, of the top view of the piezoresistive force sensor. One ion-implanted strain element is clearly visible on the right, along with the ends of the electrodes, which also serve as the mechanical mount for the beam. The beam is 0.95 mm wide by 5 mm long.

Although deadweight loading was used to a limited extent in evaluating the capacitance cell, the primary method of applying force to each device was with a nanoindenter machine (a NanoIndenter II from the MTS Nano Instruments Innovation Center). The machine's basic design and operating principles are described elsewhere [4]. Its force and displacement measuring systems are calibrated routinely at NIST. Deadweight loading is used for force calibration, and laser interferometry is used for displacement. The spring constant of the springs supporting the indenter shaft is determined by moving the shaft in air over the same range of travel used in subsequent indentation experiments. The force, displacement, and spring constant can all be determined with a relative standard uncertainty better than 1% (except for very small forces and displacements, well below the values used in this work), and extensive use at NIST has shown that precision of the force and displacement data are typically better than 0.1% for the range of values used here.

## Results

The thermal stability for both the capacitance cell and the piezoresistive sensor were evaluated by logging their output, with no force applied, for 50 h. Both devices were inside the nanoindenter enclosure, and the temperature was monitored with a platinum resistance thermometer. The results are shown in Figure 3. Both devices show drift in their output values that correlates strongly with temperature. In the case of the capacitance cell, the observed maximum variation of capacitance, 0.37 pF, is significant, amounting to an equivalent force change of 3.0 mN for a temperature variation of 0.26 °C. The piezoresistive sensor bridge output is dramatically more stable; the observed 1.03  $\mu\text{V}$  drift is the equivalent of only a 9.5  $\mu\text{N}$  force.

Both of the devices were tested by applying forces with the nanoindenter, equipped with a Berkovich diamond indenter tip. In addition, masses were also placed directly on the mass pan of the capacitance cell. The response of each device to nanoindenter loading is shown in Figures 4, 5 and 6. The nanoindenter was programmed to apply a nominal 1 mN force ten times, then a 5 mN force ten times, and finally a 10 mN force, either ten times (capacitance cell) or 5 times (piezoresistive sensor). In each case, the force was

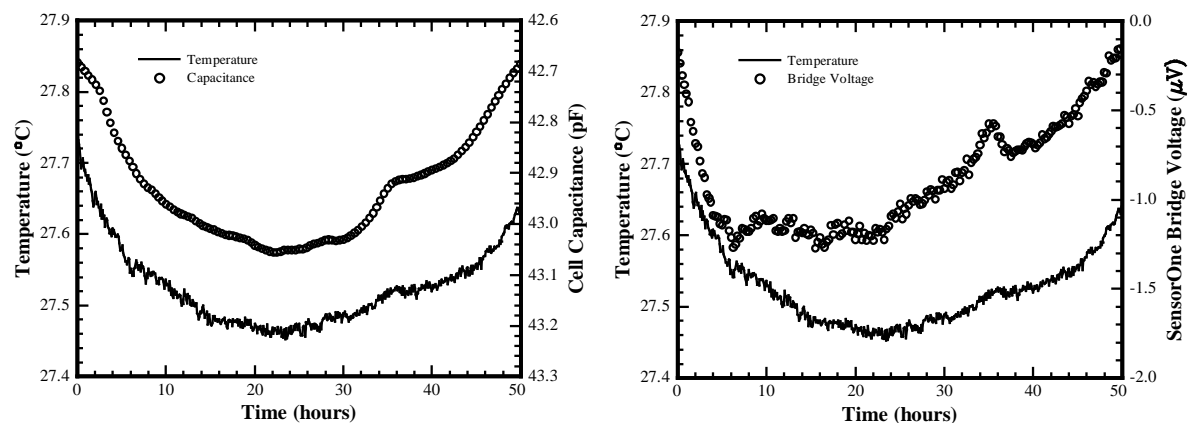


**Figure 3.** Drift in the capacitance cell (left) and piezoresistive beam (right) output over time (unloaded), each plotted with the same temperature data.

increased linearly from zero to maximum in 10 s, held at maximum for 100 s, then removed over 10 s. The small features prior to the ten 1 mN loadings in each graph are related to automated surface-finding algorithm used by the nanoindenter. The indentations were not made directly on top of one another, but were made in closely-spaced rectangular arrays, with 5  $\mu\text{m}$  spacing between nearest neighbors. Relative to the macroscopic dimensions of each device, these slight displacements are taken to be insignificant, and indeed we observe no systematic variation in response related to the relative positions of the loading points. With the capacitance cell, these arrays were made at the center of the mass pan. On the piezoresistive sensor, they were placed on the centerline of the beam, 500  $\mu\text{m}$  in from the free end.

It is clear from Figure 4 that the response of the capacitance cell is not adequately repeatable; the variation in capacitance change,  $\Delta C$ , for ten 10 mN loadings is 3.8%. There is also a substantial time-dependent response both on loading and unloading. This is shown more clearly in Figure 5, an enlargement of the 10 mN capacitance peaks from Figure 4. Capacitance continues to rise steeply (typically by over 2% of  $\Delta C$ ) after the maximum force is attained. Similar creep behavior is observed when the force is removed. Manual placement of a 1 g mass on the mass pan results in an even greater variation in capacitance change, with a strong sensitivity to slight variations in the position of the mass.

In contrast to the capacitance cell, the piezoresistive sensor showed no detectable time-dependent response to a sustained applied force, and both the mechanical and electrical response were highly reproducible over multiple applications of force. The electrical response is shown in Figure 6. The precise step height and its repeatability are shown in Table 1 for each of the three loads, and it can be seen that the electrical sensitivity of the device is relatively independent of force. The mechanical response also showed a high level of reproducibility. Figure 7 shows the force-displacement data for full loading-unloading cycles to all three maximum forces. Data from two indentations are overlaid for each maximum force. A slight hysteresis is observed between loading and unloading (the upper line and lower line, respectively, for each trace), but this is due not to mechanical hysteresis in the sensor beam, but rather to the fact that a small amount of plastic deformation of the silicon takes place at the contact point on loading that does not reverse on unloading.

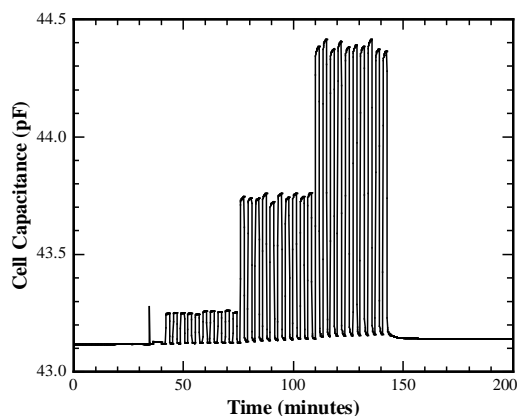


**Figure 4.** The change in capacitance of the capacitance cell for repeated loadings to nominal values of 1 mN, 5 mN and 10 mN. Note the irregular maximum values of capacitance and the shift in the baseline (zero-force) value.

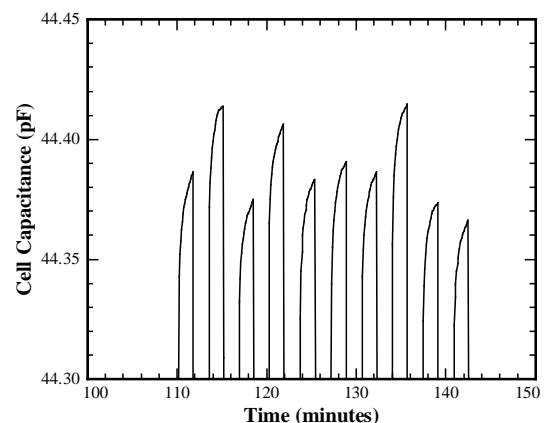


**Figure 5.** An enlargement of the 10 mN peaks from Figure 4, to emphasize the large variation in maximum capacitance for the same applied force, and show the increase in capacitance with time under maximum force.

**Table 1: Spring constant and electronic sensitivity of the SensoNor AE801 sensor element, for a 1 kHz 1.00 Vrms Wheatstone bridge drive voltage.**

Applied Force (mN)	Measured Stiffness (N/m)	Contact Stiffness (N/m)	Beam Stiffness (N/m)	Bridge $\Delta V$ ( $\mu V$ )	Sensitivity ( $\mu V/mN$ )
1.002 +/- 0.005	2085 +/- 6	$3.06 \times 10^4$	2237 +/- 7	109.2 +/- 0.5	109.0 +/- 0.5
4.888 +/- 0.004	2160 +/- 3	$6.77 \times 10^4$	2231 +/- 4	529.1 +/- 0.7	108.2 +/- 0.2
9.748 +/- 0.005	2170 +/- 2	$9.56 \times 10^4$	2220 +/- 3	1053.4 +/- 0.9	108.1 +/- 0.2

Results for the mechanical response of the beam are also presented in Table 1. The measured stiffness is calculated directly from the slope of the nanoindenter unloading data. Although approximately the same number is obtained for the beam stiffness at all three forces, there is a systematic variation of measured stiffness with applied force. This variation can in large part be explained when it is realized that the measured stiffness is in reality the series combination of the beam stiffness and the stiffness of the contact between the silicon beam and the diamond indenter tip, which depends on the contact area and is load-dependent. (The stiffness of the nanoindenter frame and the indenter shaft springs are also in the mechanical path, but these values are known from independent experiments, and the force-displacement data already incorporate those corrections.) Data from independent indentation experiments on bulk silicon were used to determine the contact stiffness between silicon and the Berkovich indenter tip for each of the applied forces used in this work, and each value of measured stiffness was corrected accordingly. The beam stiffness then obtained for each force is shown in column four of Table 1. The results, while not independent of force, vary by only 17 N/m, as compared to 85 N/m for the uncorrected stiffness.

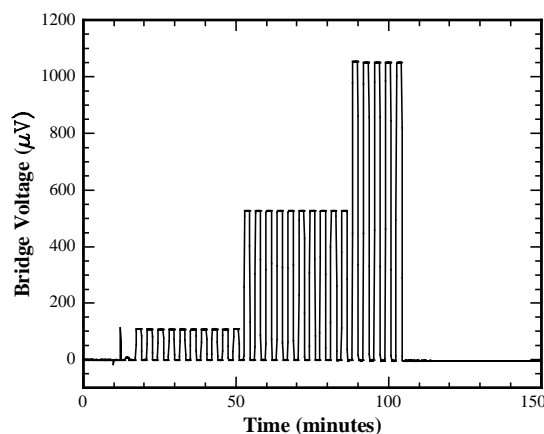


**Figure 6.** The change in bridge voltage for the piezoresistive sensor cell for repeated loadings to nominal values of 1 mN, 5 mN and 10 mN.

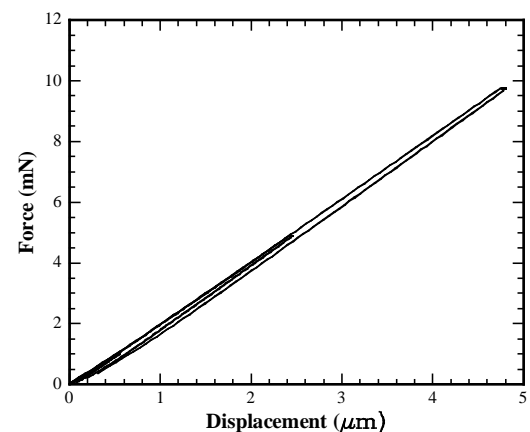


**Figure 7.** Force-displacement traces for the piezoresistive sensor, for nominal values of 1 mN, 5 mN and 10 mN maximum force. Two traces are superimposed for each force. Due to a small amount of hysteresis, the unloading data lie slightly below the loading data for each trace.

## Summary

Two devices were evaluated for possible use as force calibration load cells. The capacitance cell made of borosilicate glass was found to have unacceptably high thermal drift and creep properties. Work on the basic design will continue, however, with an emphasis on more stable mechanical assembly methods, as it is assumed at this point that the dominant source of the time-dependent behavior is the epoxy used in assembly. The piezoresistive force sensor was found to have sufficient mechanical and electrical stability for use as the basis of a force transfer standard with precision and relative uncertainty on the order of 0.1% for forces in the 1 mN to 10 mN range, sufficient for many calibration tasks in the field of micro- and nano-mechanical testing. Preliminary testing outside of this force range suggests that the useful range of the device is probably much broader.

**Disclaimer:** Certain commercial materials and equipment are identified to specify the experimental procedure. In no instance does such identification imply recommendation or endorsement by NIST or that the material or equipment identified is necessarily the best available for the purpose.

## References

- [1] D.B. Newell, J.R. Pratt, J.A. Kramar, D.T. Smith, L.A. Feeney, and E.R. Williams, Proc. Natl. Conf. of Standard Laboratories (NCSL) Intl. 2001 Workshop and Symp., Jul 29-Aug 2, 2001, Washington, D.C., Ses. 1 B.
- [2] W. Hoffmann, S. Loheide, T. Kleine-Besten, U. Brand and A. Schlachatzki, MICROtec 2000, Hannover.
- [3] J.D. Holbery, V.L. Eden, M. Sarikaya and R.M. Fisher, *Rev. Sci. Inst.* **71**[10] 3769-3776 (2000).
- [4] W.C. Oliver and G.M. Pharr, *J. Mater. Res.* **7**[6] 1564-1583 (1992).